Impacts of High Penetration of DFIG Wind Turbines on Rotor Angle Stability of Power Systems

Mohamed Edrah, Kwok L. Lo and Olimpo Anaya-Lara

***Abstract*—With the integration of wind power into power systems continues to increase, the impact of high penetration of wind power on power system stability becomes a very important issue. This paper investigates the impact of doubly fed induction generator (DFIG) control and operation on rotor angle stability. A control strategy for both the rotor-side converter (RSC) and grid-side converter (GSC) of the DFIG is proposed to mitigate DFIGs impacts on the system stability. DFIG-GSC is utilized to be controlled as static synchronous compensator (STATCOM) to provide reactive power support during grid faults. In addition, a Power System Stabilizer is implemented in the reactive power control loop of DFIG-RSC. The proposed approaches are validated on a realistic Western System Coordinating Council (WSCC) power system under both small and large disturbances. The simulation results show the effectiveness and robustness of both DFIG-GSC control strategy and power system stabilizer to enhance rotor angle stability of power system.**

***Index Terms*—Doubly fed induction generator (DFIG), power system stabilizer (PSS), rotor angle stability, STATCOM.**

I. INTRODUCTION

DUE to environmental and economic issues which progressively have become dominant issues in our society, more efforts are placed in generating electricity from renewable energy sources. Among renewable energy technologies that are being developed, wind turbine technology is the fastest growing one in the world. Variable speed wind turbines (VSWT) employing doubly fed induction generator (DFIG) is the most popular technology in currently installed wind turbines [1], [2]. With the continuous increase in penetration level of DFIG wind turbines, power system stability becomes an important issue which needs to be properly investigated.

Considerable research efforts have been dedicated to address the wind power integration issues. Reference [3] indicates that by using power electronic converters, DFIG is able to control its own reactive power to operate at a given power factor or to control the generator terminal voltage. However, the capability of DFIG voltage control cannot match that of the synchronous generator (SG) for the reason that its power converters have a limited capacity. Thus, the stability of the power system is affected in the unfortunate event that the voltage control requirement is beyond the capability of the DFIG [4]. The reactive power of DFIG can be enhanced by increasing the converters size. However, this solution increases the overall cost which is one of the main advantages of DFIG over full power converter wind turbines [5].

In [6], the effect of reactive power supplied by wind generation on rotor angle stability was examined. The study concluded that transient stability could be improved and the oscillations damped more quickly if the terminal voltage of the wind generation is controlled. Furthermore, SG rotor angle is directly influenced by reactive power control strategy used by the wind generation. However, the disturbance used in [6] is not large enough to trigger the DFIG crowbar protection system which can lead to more severe voltage sag [7]. Since keeping the DFIG connected during transient grid faults is a gird code requirement, a number of published literature [8], [9] presented various strategies to ensure the continuous operation of DFIG. In [10], a decoupled fault ride through strategy to improve inertia response and reactive power capability of DFIG is proposed. The result shows that DFIG-GSC can be used to enhance the voltage during grid fault. The used strategy in [10] prioritizes the reactive power control through the GSC over DC voltage control once the terminal voltage drops below a predefined voltage level. Moreover, the rating of the used GSC is larger than practical rating which is usually at 30% of the generator nominal power [11]. The GSC of full power converter wind turbines can also be used as STATCOM [2], [12] . This can be done at very low wind speeds or during the fault with additional devices to absorb the generated active power.

Power electronic converter of the DFIG acts as an interface between DFIG generator and the grid. Hence, with the increased penetration of DFIG, the effective inertia of the system will be reduced [13]. Therefore, since DFIGs are not synchronously coupled to the power systems, the wind turbines do not participate in electromechanical oscillations [14]. Rather, the penetration of wind power will have a damping effect due to reduction in the number of SGs that are engaged in power system oscillations. However, the effect of wind power generators on small signal stability depends on the kind of wind generator and their controllers [2]. Reference [14] stated that DFIG is able to improve power oscillations better than SG in weak systems. Moreover, VSWT are capable of controlling active and reactive power and both could be used to improve small signal stability. References [15], [16], [17] show that DFIG equipped with power system stabilizer (PSS) within active power control loop can damp the power system oscillation effectively. Consequently, DFIG with PSS

M. Edrah, K. L. Lo and O. Anaya-Lara are with the Department of Electronic and Electrical Engineering, University of Strathclyde, Glasgow, G1 1XW, U.K. (e-mail: mohamed.edrah@strath.ac.uk; k.lo@strath.ac.uk; olimpo.anaya-lara@strath.ac.uk).

can contribute to the oscillation damping much more effectively than the SG with PSS control. The control schemes used in [15], [17] are based on flux magnitude and angle control (FMAC) whilst the common control schemes for the commercial DFIG are based on standard decoupled *d-q* vector control mechanism [18]. The use of active power modulation can decrease the damping of the DFIG shaft mode [19]. This increases the stress on the DFIG rotor shaft and decreases the lifespan of the mechanical system. Moreover, reference [20] reported that PSS with active power modulation is adversely influenced by the torque variations due to tower shadow. Additionally, the effectiveness of the PSS with active power modulation can be reduced if the DFIG reactive power is used to control the grid voltage [21]. Only a small number of papers have been published concerning the use of DFIG reactive power for oscillation damping [19], [22], [23]. Also none of them take into account the influence of the crowbar system when the control of active and reactive power is lost and a large amount of reactive power is absorbed.

In this paper, a detailed analysis is carried out to study the impacts of replacing conventional SGs with equivalent DFIG wind farms on rotor angle stability of power systems. The available DFIG reactive power is utilized by two control strategies to lessen the impacts of DFIG on the rotor angle stability of the existing synchronous generators. A cost effective solution is to operate the existing DFIG-GSC as reactive power source during grid faults. Moreover, to overcome the effects of PSS power modulation, a PSS with reactive power modulation taking into account the influence of the crowbar system is designed in this paper. It is shown that the proposed technique is an efficient and effective way to improve the rotor angle stability by utilizing the available DFIG reactive power. The benefits of such control scheme could become more important as the levels of wind penetration are increased.

The paper is structured as follows: Section II describes the methodology used in this paper. Modelling and control of DFIG is described in Section III. Section IV describes the test system. The results and discussion of a number of scenarios are outlined in Section V. Finally, the paper conclusions are summarised in Section VI.

II. METHODOLOGY

In this section a methodology will be developed to study the impact of DFIG on power system rotor angle stability and its improvement.

To investigate the effect of grid connected DFIG on rotor angle stability, one of the SGs is replaced by a wind farm equipped with DFIG in the WSCC test power system. The wind farm output rating is equivalent to the replaced SG, and produces the same amount of power that is generated by the replaced SG. The topology and operating conditions of the test system with wind farm are the same prior to the SG replacement. Moreover, to evaluate the system transient response with high penetration of DFIG, the same fault is applied to the test system as in synchronous generator case.

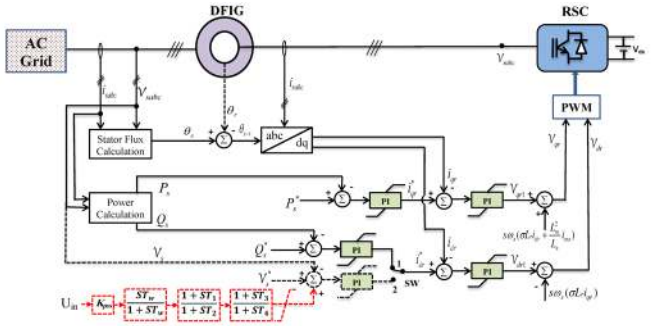

Fig. 1. Overall vector control scheme of the DFIG-RSC with voltage control (dashed black lines) and power system stabiliser (dashed red lines).

A. Small Signal Stability Analysis

The small signal stability problem usually occurs as a result of inadequate damping of one of the system rotor oscillations. The small signal stability analysis can detect system modes, which are produced by electromechanical interactions between power system SGs. Since, DFIG wind turbines are not synchronously coupled to the power systems, the wind turbines do not participate in electromechanical oscillations. However, DFIG power electronics converters have the potential to change electromechanical damping performance [10]. The methodology of small signal stability is described in the following steps:

1) Run small signal stability analysis in the frequency range of 0.1 to 2 Hz.
2) Identify the main mode that has the lowest damping factor.
3) Determine the dominant machine with its main state variables and their participation factor in the main mode.
4) Analyse the mode shape corresponding to the rotor speed state to identify generators oscillating against each other.
5) Repeat the previous steps for different scenarios.

B. Transient Stability Analysis

To conduct a transient stability analysis, the system has to be exposed to a large disturbance such as a three-phase short circuit fault. The location of the disturbance has to be chosen carefully for transient stability study. It may be selected according to the result of small signal stability study. Modes with low damping factor can be aggravated by a large disturbance. Therefore, the fault has to be near the machine that has the highest participation factor in the specified mode.

When the SGs electrical torque falls below mechanical torque during fault, the rotor will accelerate leading to a higher rotor angle position. However, for DFIG, the torque angle characteristic does not exist due to its asynchronous operation. Hence, the dynamic response of a DFIG to system disturbances is different from that of a SG [24].

The rotor angle of the interconnected SGs will be used to assess the stability of power system. Transient stability can be measured by transient stability index (TSI) which is defined as follows [25]:

$$\eta = \frac{360^{o} - \rho_{\max}}{360^{o} + \rho_{\max}} \times 100 \qquad Where \qquad -100 < \eta < 100 \tag{1}$$

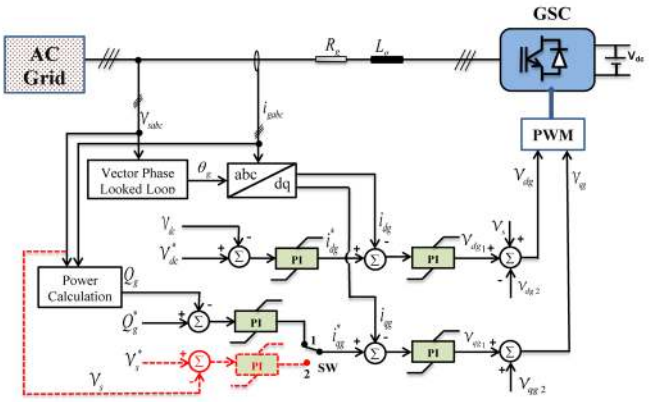

Fig. 2. Overall vector control scheme of the GSC and STATCOM mode with dashed red lines.

where η and $\rho_{\max}$ are transient stability index symbol and maximum angle separation (in degrees) between any two synchronous generators in the system at the same time respectively. The power system is considered stable if the value of η is greater than zero.

III. Modelling of DFIG Control Strategies

A. Modelling of RSC and GSC

The main objective of RSC is to regulate stator side active and reactive power independently. DFIG stator voltage can be regulated to achieve a certain limit by controlling stator reactive power through RSC. The voltage control outer loop is marked in dashed black lines in Fig.1. The rotor side power converter can be modelled as a current controlled voltage source converter [11]. The control of DFIG stator active power P_s and reactive power Q_s is achieved by controlling the rotor current i_{rabc} in in *d-q* reference frame. The detailed model of RSC that is adopted in this paper can be found in [26], [27].

The main objective of GSC is to control the voltage of the DC link to maintain it within a certain limit. However, it can regulate the reactive power that GSC can exchange with the grid and can be used as a reactive power support [28].

The overall vector control scheme of the GSC is shown in Fig. 2, in which the stator current i_{gabc} in the synchronous rotating reference frame is used to control the DC voltage (v_{dc}) and the reactive power Q_g. The detailed model of DFIG-GSC that is used in this paper can be found in [26], [27].

B. Modelling of GSC as STATCOM

When the terminal voltage at the DFIG decreases rapidly to a low level, the machine fluxes are forced to change suddenly leading to high rotor currents. These currents can damage the DFIG-RSC. Therefore, in modern wind turbines, DFIG crowbar system is activated when overcurrent exists in the rotor windings. The crowbar system consists of a set of three-phase series resistance connected to the rotor windings [10].

Following the short circuit, the crowbar will be activated and hence the DFIG will work as a squirrel cage induction generator. In this case, a large amount of reactive power will

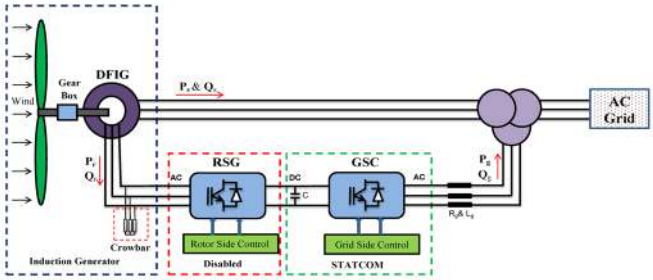

Fig. 3. General structure of modelling DFIG-GSC as STATCOM.

be absorbed from the grid by the induction generator. The crowbar resistance should be high enough to limit the short circuit rotor current and it should be low enough to avoid too high voltage in the rotor circuit. Therefore the crowbar resistance must be chosen carefully. After the fault is cleared out, a delay time between 60 ms to 120 ms is needed to allow the machine flux transients to die down. Then the crowbar can be switched off and the RSC goes back to control the DFIG [29].

Since the RSC is deactivated during large transient disturbances, the GSC can be used as a STATCOM, as can be seen in Fig. 3, to produce reactive power. The GSC is similar to the traditional voltage source converter (VSC) based STATCOM which consists of a VSC and a DC capacitor. The control system of STACOM is based on the standard *d-q* vector control scheme. The main objective of the STATCOM control circuit is to maintain the voltage of the DC capacitor constant and to regulate the interchanged reactive power between the converter and the grid. The detailed model of STATCOM can be found in [30], [31]. The control circuit of STATCOM is very similar to that already installed in the GSC. The same DC voltage control loop which maintains the DC voltage constant in GSC can be used without any modification to maintain the DC voltage of the STATCOM constant. The reactive power control loop which controls reactive power flowing between the grid and the GSC can be used without any change to produce maximum reactive power of the GSC. It can also be used to regulate the DFIG terminal voltage when the switch (SW) is in position 2 in Fig. 2.

During normal operation conditions, the RSC controls independently the stator active and reactive power, whilst the GSC independently controls the DC voltage and the exchange of reactive power between the GSC and the grid. The GSC is usually operated at a unity power factor to allow the rated rotor slip power to be exchanged through the converter. When the crowbar is activated, the rotor windings are short circuited through the crowbar impedance and the RSC is deactivated. Since the GSC is decoupled from the rotor windings, there is no need for it to be disabled and hence can be used as STATCOM as long as the RSC is deactivated. The necessary time for the RSC to be blocked can be less than 1 ms [2]. Therefore, once the crowbar is triggered the set point of the GSC reactive power ($Q^*_{g)}$ can be changed to 1 pu to deliver its maximum reactive power or change the position of the switch (SW) to position 2 to regulate the terminal voltage. The

reactive power that can be delivered from STATCOM mode is limited by the rating of GSC which is about 30% of DFIG rating. The synchronization of the RSC can be established after the fault and during the crowbar active time. When the crowbar is deactivated, the RSC is activated and the set point of the GSC reactive power is set back to zero or change the switch position back to 1 for normal operation condition.

C. *Modelling of power system stabilizer*

The aim of this section is to model a PSS for DFIG based wind farm to enhance the test system stability and to damp rotor angle oscillations. Designing a PSS for DFIG has to take into account that the DFIG does not introduce any new oscillation modes to the system. The main function of PSS is to damp low frequency oscillations in the range of 0.1 to 2 Hz, which are known as inter area or local modes. The input signal of PSS can be any signal affected by the oscillation such as machine speed, grid frequency, terminal voltage and oscillating power. In this study, a local signal is carefully chosen as PSS input signal to avoid the use of wide area communications.

The location of the measurement point is very important for the controller. The point of common coupling (PCC) of the wind farm is a favourable selection point to avoid filtering effect of transformers between the grid and the wind farm. The best input signals reported in [32] are voltage and frequency. Conversely other signals are less sensitive to system oscillations and hence cannot provide adequate information about oscillatory modes to be damped by the PSS. The conventional PSS with lead-lag controllers is represented by equation (2) [33].

$$u_{pss} = K_{pss}\left(\frac{ST_w}{1+ST_w}\right)\left(\frac{1+ST_1}{1+ST_2}\right)\left(\frac{1+ST_3}{1+ST_4}\right)u_{in} \quad (2)$$

where, u_{in} and u_{pss} are control input and output signals respectively, K_{pss} is the controller gain, T_w is a washout time constant (s) and T_1 to T_4 are lead-lag time constants (s).

Since the DFIG is partly decoupled from the grid by the partially rated converters, the power and rotational speed signals are less sensitive to grid oscillations. Moreover, these signals are influenced by torque variations due to tower shadow. Therefore, the available local signals such as local bus voltage and frequency are examined using residue analysis. The residue of a particular mode can provide clear measures of the mode's sensitivity to the selected PSS input signal. Based on the residue analysis, network frequency is selected as best local signal for successfully damping oscillations. The PSS output signal is added to the reference voltage signal in the RSC as can be seen with the red dashed lines in Fig. 1. The amount of damping is determined by the PSS gain (K_{pss}). Washout block is a high pass filter that allows a selected input frequency range and expected to act only during transient period. The dynamic phase compensator can provide a lead or lag phase in order to reduce rotor angle oscillations. Limiter is used to prevent output signal from exceeding control limits. The PSS output limit is set to ±0.1 pu in this study. Parameters of the PSS are given in the following equation.

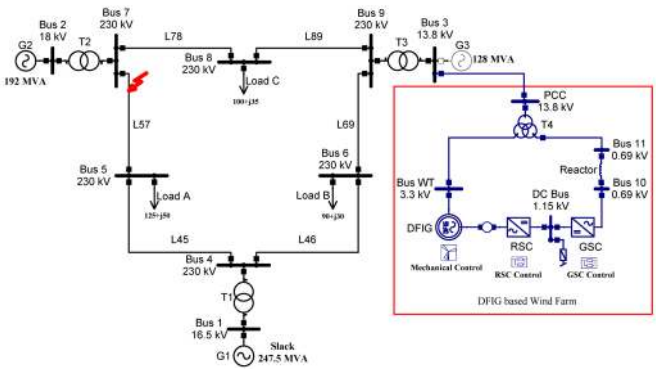

Fig. 4. Single line diagram of the test system with DFIG based wind farm.

$$u_{pss} = 170\left(\frac{5S}{1+5S}\right)\left(\frac{1+0.06308S}{1+0.26497S}\right)\left(\frac{1+0.06308S}{1+0.26497S}\right)u_{in} \quad (3)$$

IV. TEST SYSTEM

The standard Western System Coordinating Council (WSCC) 3-generators 9-buses test system is used to study the impact of DFIG wind turbine on power system rotor angle stability as shown in Fig. 4. The system consists of three synchronous generators with three fixed-tap step-up transformers, six transmission lines and three loads totalling 315 MW and 115 MVAr. The three SGs are equipped with an IEEE type 1 exciter. However, the three generators were not equipped with PSS for more straightforward assessment. The synchronous machines G_1 and G_2 are equipped with turbine governor type TGOV1. The static and dynamic data of the test system can be found in [34].

To investigate the effect of DFIG based wind farm on the power system rotor angle stability, a DFIG wind farm is connected to the test system. Both the test system and wind farm are modelled in details and simulated by using NEPLAN software [35]. The DFIG controls are modelled in the simulation tool as described in Section III. The three loads were modelled as nonlinear ZIP loads (33% constant current *I*, 33% constant power *P* and 33% constant impedance *Z*) [36].

A wind farm may consist of a large number, between (10 - 100s), of individual DFIG wind turbines. Representing each wind turbine of the wind farm in the simulation tool increases system complexity and simulation time. Therefore, an aggregation method can be applied to reduce the large number of wind turbines and to make the system simpler. In this study, the aggregation method used is explained in [37]. The DFIG that represents the aggregated DFIG based wind farm is shown in Fig. 4. The 85 MW wind farm was aggregated from 17 turbines of 5 MW each to achieve an equivalent generated power to replace synchronous generator G_3. Hence, the generated power from DFIG wind farm is accounted as 27% of the total consumed power of the test system.

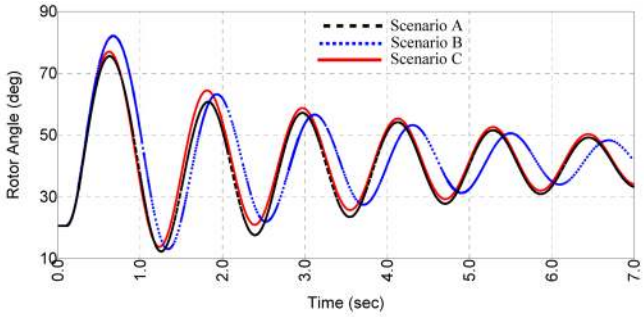

Fig. 5. Rotor angle of G_2 for scenarios (A-C).

TABLE I
MAIN ELECTROMECHANICAL MODES OF SCENARIOS A- C

Scenarios	A	B	C
Eigenvalue $\lambda = \sigma + j\omega$ (pu)	-0.265 ±j7.615	-0.297±j7.778	-0.306 ± 7.734
Frequency f (Hz)	1.212	1.238	1.231
Damping Factor ζ (%)	3.5	3.8	3.9
Dominant variable	ρ, ω	ρ, ω	ρ, ω
Dominant Machine	G_2	G_2	G_2
Participation factor (%)	35.8, 37.5	40.3, 42.1	40.2, 42.3

V. Results and Discussion

The simulation studies carried out in this section are based on the methodology described in Section II. In this paper, five different scenarios are analysed by small signal and transient stability to show the impact of DFIG on power systems rotor angle stability and how the disturbance can be mitigated by the proposed control strategies. The description of each case is as following:

- **Scenario A**: synchronous generator (SG) scenario. It is a base case scenario in which the three generators are conventional synchronous generators.
- **Scenario B**: fixed unity power factor (PF) control mode (no reactive power injected to the system from DFIG). In this scenario G_3 is replaced by DFIG based wind farm with a PF control mode.
- **Scenario C**: voltage control (VC) mode. The wind farm operates to maintain its terminal voltage at 1pu. In this scenario G_3 is replaced by DFIG based wind farm with a voltage control mode.
- **Scenario D**: STATCOM control mode. The proposed use of DFIG-GSC as STATCOM control strategy will be investigated in this scenario.
- **Scenario E**: DFIG power system stabilizer. The DFIG will be equipped with the proposed PSS.

Scenarios A-C

A detailed small signal stability study on the test system was conducted for the first three scenarios. The rotor angle oscillations in the frequency range of 0.1 to 2 Hz are monitored. The dominant electromechanical mode for each scenario can be seen in Table I. The test system is stable and the main modes of three scenarios are dominated by rotor angle ρ and speed ω of generator G_2. The frequency of each mode is relatively similar in the three scenarios. The damping factor of the main mode is improved from 3.5% (scenario A) to 3.9% (scenario C). Moreover, contribution of G_2 to the oscillatory modes in DFIG scenarios is higher than the first scenario.

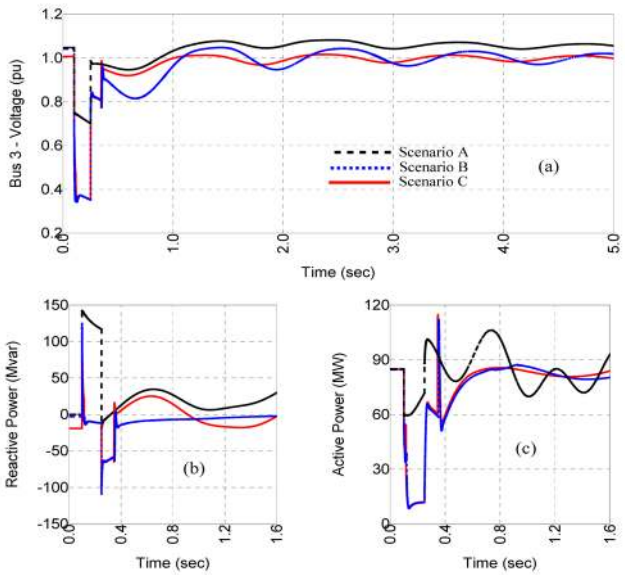

Fig. 6. Transient responses of the studied system, (a) Generator's terminal voltage (Bus 3), (b) Generator's total reactive power, (c) Generator's total active power.

For more detailed analysis, mode shape that corresponding to the rotor speed state variable for the three scenarios is examined. In first scenario, the results indicate that the three synchronous generators of the test system are participating in the mode, where G_1 is oscillating against the other two. But when G_3 is replaced by DFIG, the wind farm does not contribute to the mode. The mode gets the contribution from G_1 and G_2 which are oscillating against each other.

The result of small signal stability study shows G_2 has the highest participation factor. Therefore, according to the methodology described in Section II, the location of the disturbance has to be near G_2. A disturbance lasting 9-sycle (150 ms) of a 3-phase to ground fault at 60 Hz was imposed near Bus 7 on line 5-7. The fault was cleared by opening both sides of the faulted line simultaneously.

In order to assess the effect of DFIG based wind farm on transit stability of the test system, rotor angle of each generator is observed, from which the transient stability index is calculated. Active and reactive power output of each generator is monitored. Moreover, terminal voltage of the replaced synchronous generator (Bus 3) is monitored. The angle of the largest synchronous generator G_1, which is the slack generator, was taken as a reference angle.

In Fig. 5, rotor angle oscillation of the G_2 relevant to G_1 can be seen for the three scenarios. The figure shows that rotor angle variation of the system in scenario B has a larger rotor angular swing than that in the first scenario. However, the rotor angular swing is improved when wind farm controls its terminal voltage. This indicates that controlling the reactive power of the wind farm to achieve a predefined voltage value can improve rotor angle stability.

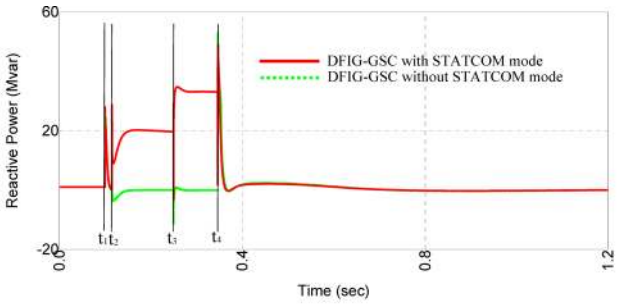

Fig. 7. Reactive power of DFIG-GSC during normal operation (dotted green line) and STATCOM modes (red line).

TABLE II
TRANSIENT STABILITY INDEX OF SCENARIOS A-C

TSI	Scenario A	Scenario B	Scenario C
η	65.3	62.87	64.77

TABLE III
TRANSIENT STABILITY INDEX OF SCENARIO D

TSI	PF	VC
η	63.55	65.38

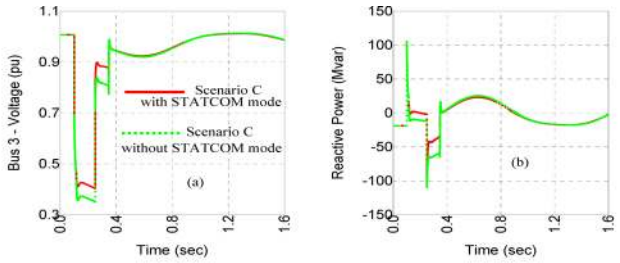

Fig. 8. (a) DFIG terminal voltage and (b) DFIG reactive power with and without STATCOM mode.

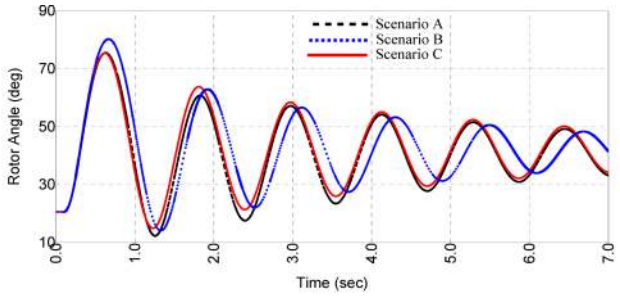

Fig. 9. Rotor angle of G_2 for scenario D.

Table II shows that the stability of the test system is reduced after synchronous generator G_3 is replaced by a wind farm operating at a unity power factor. However, DFIG with voltage control mode improves G_2 rotor angle.

Terminal voltage of G_3 falls to about 0.7 pu during the fault period and then recovered quickly to its normal value after the fault is cleared as indicated in Fig. 6(a). However, in the case of wind farm, the terminal voltage falls to 0.4 pu during the fault period and then recovers to about 0.8 pu after fault clearance when the crowbar is still active. During the active crowbar time the induction generator absorbs a large amount of reactive power as can be seen in Fig. 6(b). In comparison to the scenario B, the terminal voltage of wind farm in scenario C recovers more quickly to its predefined value after the crowbar is deactivated. This is due to the reactive power that is injected into the grid to maintain the terminal voltage of the wind farm at its nominal value. Moreover, there is more reactive power injected into the grid in the SG case than that is injected by the wind farm. This is due to the ability of the SG to inject reactive power over the whole fault period.

Active power of G_3 and DFIG based wind farm for each scenario can be seen in Fig. 6(c). The active power produced by DFIG in voltage control scenario is similar to the unity power factor scenario. However, the active power of wind farm scenarios and SG scenario are different during and after the fault is cleared. Synchronous generator G_3 is providing the grid with about 60 MW of active power during the fault period compared to just 12 MW injected from the wind farm. The active power of G_3 after the fault oscillates because of its rotor inertia response. But in the case of wind farm, the active power output after the fault is relatively smooth.

The analysis and simulation results of previous scenarios clearly show that replacing synchronous generator with DFIG based wind farm has no negative impacts on small signal stability of power systems. However, the impacts on transient stability of the system would depend on the control strategy used within the DFIG-RSC. The results of completed analysis demonstrate that although DFIG with voltage control can produce reactive power after crowbar deactivation time, both of control modes (PF and VC) cannot provide any reactive power during crowbar active time. On the contrary, DFIG absorbs a large amount of reactive power leading to a severe voltage drop. In the next scenario, STATCOM control mode will be used within the DFIG-GSC to supply some of the reactive power absorbed by the induction generator during disturbances and hence improves wind farm terminal voltage.

Scenario D: STATCOM control mode

Fig. 7 shows the amount of reactive power that can be delivered from DFIG-GSC during normal operation and STATCOM mode. In the case of normal operation, GSC cannot provide any reactive power support during fault. In this case the GSC has no contribution towards transient stability improvement. However, in the case of STATCOM mode, GSC provides reactive power support during and after the fault when the DFIG crowbar is still active. The same 3-phase short-circuit fault as stated in previous scenarios is applied at (t_1 = 0.1 s). The DFIG crowbar is triggered at (t_2 = 0.12 s) to initiate the STATCOM mode after few milliseconds. During the fault period, the DFIG-GSC provides about 20 MVAr which helps to improve the terminal voltage of DFIG wind farm. The wind farm terminal voltage is improved from 0.37 pu to 0.42 pu with STATCOM mode during the fault as shown in Fig. 8(a). Although, the fault is cleared at (t_3 = 0.25 s), the STATCOM mode is deactivated at (t_4 = 0.35 s) when the DFIG crowbar system is also deactivated. After the fault, DFIG-GSC provides its full rated reactive power to support the terminal voltage of wind farm. The terminal voltage of the wind farm recovers from 0.81 pu to 0.88 pu with STATCOM mode. Fig. 8(b) clearly shows that with STATCOM mode less reactive power is absorbed from the grid.

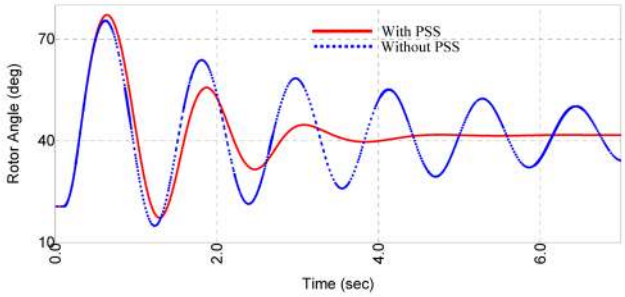

Fig. 10. Rotor angle of G_2 for scenario (E).

TABLE IV
MAIN ELECTROMECHANICAL MODE OF SCENARIO E

Scenarios	E
Eigenvalue $\lambda = \sigma + j\omega$ *(pu)*	-0.967 ± 7.964
Frequency f(Hz)	1.268
Damping Factor ζ (%)	12
Dominant variable	ρ, ω
Dominant Machine	G_2
Participation factor (%)	48.3, 50.8

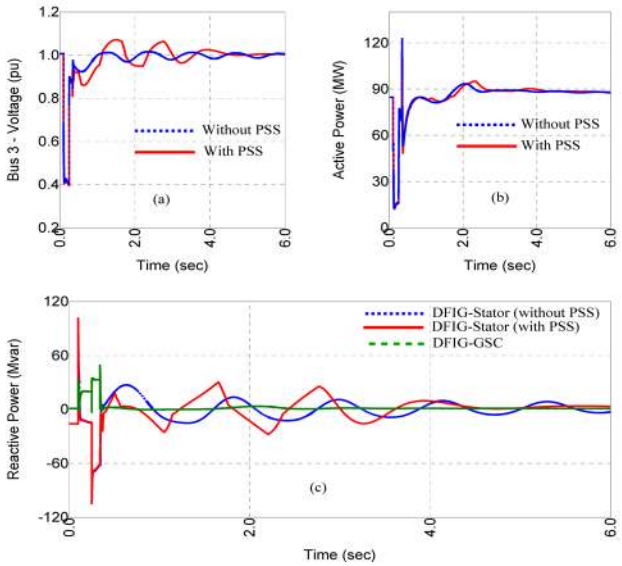

Fig. 11. (a) DFIG terminal voltage, (b) DFIG active power, (c) DFIG stator and GSC reactive power.

Fig. 9 presents the rotor angle of G_2 when STATCOM mode is used. The magnitude of the rotor angles in scenarios B&C is slightly lower when it is compared to those in Fig. 5. A smaller rotor angle deviation of G_2 has been gained in the case of STATCOM mode. The rotor angle magnitude and oscillation in the case of DFIG voltage control mode with STATCOM mode performs as good as if not better when compared to synchronous generator scenario. Therefore, replacing a SG by DFIG based wind farm controlling its terminal voltage and equipped with STATCOM mode has no negative impacts on the transient stability of the power system. Moreover, this result is also reinforced by the transient stability index as shown in Table III. Once again, the stability index of scenarios B&C is improved from 62.87 and 64.77 (Table II) to 63.55 and 65.38 (Table III) respectively. It should be noticed that the VC mode with STATCOM mode has better stability index (65.38) than the SG case (65.3).

The results of this scenario indicate that transient stability of the system is improved by using DFIG-GSC as STATCOM. The reactive power provided by STATCOM mode improves the terminal voltage of wind farm during the disturbance and hence resulting in better system stability. Since the terminal voltage of DFIG based wind farm can be controlled by the voltage control strategy of RSC during normal operation conditions, the STATCOM mode can provide a voltage support during transient periods when the crowbar is active.

Scenario E: DFIG power system stabilizer

In this scenario, the proposed model of power system stabilizer in Section III is examined. The PSS is attached to a DFIG based wind farm with both voltage control strategy and STATCOM mode. As can be seen in Table IV, once again, the main modes of three scenarios are dominated by rotor angle ρ and speed ω of generator G2. However, the system is much more stable in this scenario than all previous scenarios. Rotor angle stability of the system is improved due to the effectiveness of the proposed PSS. The damping factor of the main mode is increased significantly from 3.9% (without PSS) to 12% (with PSS).

Dynamic response of rotor angle of G_2 with and without PSS is shown in Fig. 10. The time domain simulation clearly shows the oscillation damps quickly and the rotor angle steady state value is reached in a time of less than 4 s. Therefore, it is clear that DFIG based wind farm has the capability to improve rotor angle oscillations.

Since PSS output signal is connected to the reactive power loop, the difference between the two cases (with and without PSS) is only in the reactive power output as can be seen in Fig. 11. This is apparent only after the fault is cleared and when the PSS is activated to damp the rotor angle oscillations. After the fault is cleared the terminal voltage of the wind farm with PSS is more variable, as shown in Fig. 11(a), due to the reactive power variation. However, this variation is limited and is effectively damped in 4 s.

DFIG based wind farms equipped with PSS can use STATCOM mode to improve system transient stability. In a similar way to scenario D, the GSC can be used as a reactive power support during the time when DFIG crowbar is active. Fig. 11(c) shows the reactive power output of the STATCOM mode when the wind farm is equipped with PSS. The GSC provides a reactive power support during the time when DFIG crowbar is active. Conversely, the PSS starts to control the DFIG stator reactive power after the crowbar is deactivated.

Based on the results of this scenario, DFIG based wind farms can damp rotor angle oscillation effectively by using a PSS attached to the DFIG-RSC reactive power control loop. Moreover, the transient stability results indicate that the DFIG-GSC control strategy can be used on the same DFIG based wind farm that is fitted with PSS to improve transient stability of the power system.

VI. Conclusions

In this paper, the impact of high penetration of DFIG based wind farm on rotor angle stability has been investigated. From the results of this study, it is clear that replacing conventional SGs with equivalent DFIG wind farms have negative impacts on rotor angle stability of power systems. However, theses impacts can be mitigated by the proposed control strategies and hence the penetration of wind power can be increased without degrading the rotor angle stability. The use of GSC as STATCOM is a cost effective solution to support local voltage of wind farms without an external STATCOM. Moreover, the implementation of the proposed PSS within the reactive power control loop of the wind farm can influence the rotor angle of SG and thus damp the power system oscillations effectively. As the levels of wind penetration are increased, the benefit of such control scheme is that the DFIG based wind farms are able to take over the SGs responsibility to support power system stability.

References

[1] F. Blaabjerg and M. Ke, "Future on Power Electronics for Wind Turbine Systems," *Emerging and Selected Topics in Power Electronics, IEEE Journal of,* vol. 1, pp. 139-152, 2013.

[2] T. Ackermann, *Wind Power in Power Systems*: John Wiley & Sons, 2012.

[3] W. Feng, Z. Xiao-Ping, K. Godfrey, and J. Ping, "Modeling and Control of Wind Turbine with Doubly Fed Induction Generator," in *Power Systems Conference and Exposition, 2006. PSCE '06. 2006 IEEE PES*, 2006, pp. 1404-1409.

[4] M. J. Hossain, H. R. Pota, M. A. Mahmud, and R. A. Ramos, "Investigation of the Impacts of Large-Scale Wind Power Penetration on the Angle and Voltage Stability of Power Systems," *Systems Journal, IEEE,* vol. 6, pp. 76-84, 2012.

[5] R. Cardenas, R. Pena, S. Alepuz, and G. Asher, "Overview of control systems for the operation of DFIGs in wind energy applications," *IEEE Transactions on Industrial Electronics,* vol. 60, pp. 2776-2798, 2013.

[6] E. Vittal, M. O'Malley, and A. Keane, "Rotor Angle Stability With High Penetrations of Wind Generation," *Power Systems, IEEE Transactions on,* vol. 27, pp. 353-362, 2012.

[7] G. Pannell, D. J. Atkinson, and B. Zahawi, "Minimum-threshold crowbar for a fault-ride-through grid-code-compliant DFIG wind turbine," *Energy Conversion, IEEE Transactions on,* vol. 25, pp. 750-759, 2010.

[8] A. H. Kasem, E. F. El-Saadany, H. H. El-Tamaly, and M. A. A. Wahab, "An improved fault ride-through strategy for doubly fed induction generator-based wind turbines," *Renewable Power Generation, IET,* vol. 2, pp. 201-214, 2008.

[9] A. D. Hansen and G. Michalke, "Fault ride-through capability of DFIG wind turbines," *Renewable Energy,* vol. 32, pp. 1594-1610, 2007.

[10] L. G. Meegahapola, T. Littler, and D. Flynn, "Decoupled-DFIG Fault Ride-Through Strategy for Enhanced Stability Performance During Grid Faults," *Sustainable Energy, IEEE Transactions on,* vol. 1, pp. 152-162, 2010.

[11] R. Pena, J. Clare, and G. Asher, "Doubly fed induction generator using back-to-back PWM converters and its application to variable-speed wind-energy generation," *IEE Proceedings-Electric Power Applications,* vol. 143, pp. 231-241, 1996.

[12] T. H. Nguyen and D.-C. Lee, "Advanced fault ride-through technique for PMSG wind turbine systems using line-side converter as STATCOM," *Industrial Electronics, IEEE Transactions on,* vol. 60, pp. 2842-2850, 2013.

[13] J. G. Slootweg and W. L. Kling, "The impact of large scale wind power generation on power system oscillations," *Electric Power Systems Research,* vol. 67, pp. 9-20, 2003.

[14] G. Tsourakis, B. M. Nomikos, and C. D. Vournas, "Contribution of Doubly Fed Wind Generators to Oscillation Damping," *Energy Conversion, IEEE Transactions on,* vol. 24, pp. 783-791, 2009.

[15] Y. Mishra, S. Mishra, M. Tripathy, N. Senroy, and Z. Y. Dong, "Improving Stability of a DFIG-Based Wind Power System With Tuned Damping Controller," *Energy Conversion, IEEE Transactions on,* vol. 24, pp. 650-660, 2009.

[16] M. Zhixin, F. Lingling, D. Osborn, and S. Yuvarajan, "Control of DFIG-Based Wind Generation to Improve Interarea Oscillation Damping," *Energy Conversion, IEEE Transactions on,* vol. 24, pp. 415-422, 2009.

[17] F. M. Hughes, O. Anaya-Lara, N. Jenkins, and G. Strbac, "A power system stabilizer for DFIG-based wind generation," *Power Systems, IEEE Transactions on,* vol. 21, pp. 763-772, 2006.

[18] S. Muller, M. Deicke, and R. W. De Doncker, "Doubly fed induction generator systems for wind turbines," *Industry Applications Magazine, IEEE,* vol. 8, pp. 26-33, 2002.

[19] F. Lingling, Y. Haiping, and M. Zhixin, "On Active/Reactive Power Modulation of DFIG-Based Wind Generation for Interarea Oscillation Damping," *Energy Conversion, IEEE Transactions on,* vol. 26, pp. 513-521, 2011.

[20] F. M. Hughes, O. Anaya-Lara, G. Ramtharan, N. Jenkins, and G. Strbac, "Influence of Tower Shadow and Wind Turbulence on the Performance of Power System Stabilizers for DFIG-Based Wind Farms," *Energy Conversion, IEEE Transactions on,* vol. 23, pp. 519-528, 2008.

[21] M. Edrah, K. L. Lo, A. Elansari, and O. Anaya-Lara, "Power oscillation damping capabilities of doubly fed wind generators," in *Power Engineering Conference (UPEC), 2014 49th International Universities*, 2014, pp. 1-6.

[22] Y. Haiping, F. Lingling, and M. Zhixin, "Reactive power modulation for inter-area oscillation damping of DFIG-based wind generation," in *Power and Energy Society General Meeting, 2010 IEEE*, 2010, pp. 1-9.

[23] R. D. Fernandez, R. J. Mantz, and P. E. Battaiotto, "Contribution of wind farms to the network stability," in *Power Engineering Society General Meeting, 2006. IEEE*, 2006, p. 6 pp.

[24] F. M. Hughes, O. Anaya-Lara, N. Jenkins, and G. Strbac, "Control of DFIG-based wind generation for power network support," *Power Systems, IEEE Transactions on,* vol. 20, pp. 1958-1966, 2005.

[25] L. Shi, S. Dai, Y. Ni, L. Yao, and M. Bazargan, "Transient stability of power systems with high penetration of DFIG based wind farms," in *Power & Energy Society General Meeting, 2009. PES'09. IEEE*, 2009, pp. 1-6.

[26] Q. Wei, G. K. Venayagamoorthy, and R. G. Harley, "Real-Time Implementation of a STATCOM on a Wind Farm Equipped With Doubly Fed Induction Generators," *Industry Applications, IEEE Transactions on,* vol. 45, pp. 98-107, 2009.

[27] L. Qu and W. Qiao, "Constant power control of DFIG wind turbines with supercapacitor energy storage," *Industry Applications, IEEE Transactions on,* vol. 47, pp. 359-367, 2011.

[28] E. Tremblay, A. Chandra, and P. Lagace, "Grid-side converter control of DFIG wind turbines to enhance power quality of distribution network," in *Power Engineering Society General Meeting, 2006. IEEE*, 2006, p. 6 pp.

[29] I. Erlich, H. Wrede, and C. Feltes, "Dynamic Behavior of DFIG-Based Wind Turbines during Grid Faults," in *Power Conversion Conference - Nagoya, 2007. PCC '07*, 2007, pp. 1195-1200.

[30] P. Rao, M. L. Crow, and Y. Zhiping, "STATCOM control for power system voltage control applications," *Power Delivery, IEEE Transactions on,* vol. 15, pp. 1311-1317, 2000.

[31] S. Li, L. Xu, and T. A. Haskew, "Control of VSC-based STATCOM using conventional and direct-current vector control strategies," *International Journal of Electrical Power & Energy Systems,* vol. 45, pp. 175-186, 2013.

[32] A. Mendonca and J. A. P. Lopes, "Robust tuning of power system stabilisers to install in wind energy conversion systems," *Renewable Power Generation, IET,* vol. 3, pp. 465-475, 2009.

[33] M. A. Abido, "A novel approach to conventional power system stabilizer design using tabu search," *International Journal of Electrical Power & Energy Systems,* vol. 21, pp. 443-454, 1999.

[34] P. M. Anderson and A. A. Fouad, *POWER SYSTEM CONTROL AND STABILITY*: Wiley-IEEE Press 2003.

[35] B. Busarello. *Cott+ Partner AG,"NEPLAN, power system analysis,"* Available: www. neplan. ch

[36] "Standard load models for power flow and dynamic performance simulation," *Power Systems, IEEE Transactions on,* vol. 10, pp. 1302-1313, 1995.

[37] M. PŸller and S. Achilles, "Aggregated wind park models for analyzing power system dynamics," 2003.